in Equation (29). This cannot be true as $\bar{P}$ approaches zero, for then ΔP is not negligible with respect to P.

SUMMARY

The method developed for calculating flow and diffusion for a binary system contains no arbitrary constants when applied to a single capillary. For the special case of a pure component system, agreement between experimental and predicted results is good. To apply the method to porous media requires a model of the pore structure. This problem is taken up in Part II.

ACKNOWLEDGMENT

This work was possible because of the financial support of the National Science Foundation. The assistance of Mr. H. Izawa in the experimental work is acknowledged.

NOTATION

a = radius of cylindrical capillary or pore, cm.
C_A = concentration of component A, g. moles/cc.
C = flow parameter for a single capillary, defined by Equation (15), sq.cm./sec.
D_{AB} = bulk diffusivity in binary gas mixture A-B, sq. cm./sec.
D_{KA} = Knudsen diffusivity of gas A, sq.cm./sec.
F = flux due to a pressure difference, g. moles/(sec.)(sq.cm.); F_{sf} = slip flow contribution
M = molecular weight
m = $(M_A/M_B)^{1/2}$
N_A = flux of component A, g. moles/(sec.)(sq.cm.)
N_A° = diffusion flux of A, that is flux of A under constant pressure diffusion conditions, g. moles/(sec.)(sq.cm.)
P = total pressure, dynes/(sq. cm.)
R = gas constant, dyne (cm.)/(g. mole)(°K.)
T = temperature, °K.
T_o = flow rate per unit pressure drop, defined by Equation (28), cc./sec.
$\bar{v}$ = mean molecular speed, cm./sec.
x = distance in direction of diffusion, cm.
y = mole fraction of gas
Φ = probability of a molecule to be in Knudsen flow; Φ_s is defined by Equation (26), Φ_N by Equation (23)
μ = gas viscosity, poises
λ = mean free path, cm.

LITERATURE CITED

1. Bosanquet, C. H., *British TA Rept. BR-507* (Sept. 27, 1944).
2. Evans, R. B., III, G. M. Watson, and E. A. Mason, *J. Chem. Phys.*, **35**, 2076 (1961).
3. *Ibid.*, **36**, 1894 (1962).
4. Kennard, E. H., "Kinetic Theory of Gases," McGraw-Hill, New York (1938).
5. Knudsen, M., *Annalen der Physik*, **28**, 75 (1909).
6. Pollard, W. G., and R. D. Present, *Phys. Rev.*, **73**, 762 (1948).
7. Rothfeld, L. B., *A.I.Ch.E. Journal*, **9**, 19 (1963).
8. Scott, D. S., and F. A. L. Dullien, *ibid.*, **8**, 113 (1962).
9. *Ibid.*, 293.
10. Weber, Sophus, *Kgl. Danske Videnskab. Selskab., Mat.-fys. Medd.*, **28**, No. 2 (1954).

Part II. Diffusion and Flow in Porous Catalysts

SEIYA OTANI, NORIAKI WAKAO, and J. M. SMITH

Diffusion and flow rates through porous catalysts were measured under the conditions of finite pressure gradients for single- and two-component systems. For large pore (low density) alumina pellets the diffusion rate counter to the pressure gradient was severely depressed, while for small pore Vycor the pressure gradient had little effect.

The equations developed in Part I for flow and diffusion in a single capillary were extended to porous catalysts. The resulting prediction methods contain no parameters which require transport data for their evaluation, but pore size and void fraction information is needed. For the catalysts investigated, both the permeability and diffusion rates varied several thousand-fold. The calculated results predict the same extensive range and show the same effects of pressure gradient and pore properties. Also the quantitative agreement between calculated and experimental results is such that the theory provides a useful method of predicting transport rates through certain types of porous media.

The objective of this part of the paper is the measurement of diffusion rates, both counter to and in the direction of enforced pressure gradients, through typical porous catalysts. Also consideration is given to the prediction of diffusion and flow rates from easily measured, geometrical properties of the catalysts. In Part I equations were derived for a single capillary so that the objective here is to adapt the results to porous materials typical of solid catalysts. A random pore concept has been used (4) to treat the constant pressure case. The same model will be used in this part for diffusion and flow with a pressure gradient. The treatment is restricted to an isothermal binary system of gases A and B. The authors consider a pellet of thickness L across which diffusion and flow occur in one dimension. One face is exposed to gas A at a constant pressure P_1 and the other to B at a lower, constant pressure P_2. The problem is to determine the molal fluxes of A and B.

Flow of pure A through the same pellets was also measured and predicted by adapting the permeability equations of Part I.

EXPERIMENTAL METHOD AND APPARATUS

The permeability measurements were made with nitrogen supplied to both sides of the pellet chamber (8) as shown in Figure 1. For diffusion studies nitrogen and hydrogen were chosen to avoid surface effects and to utilize the large diffusivity of hydrogen. The apparatus was operated at pressures from

1.0 to 10 atm., with pressure gradients across the pellet ranging from 0 to 5 atm. The temperature was approximately 25°C.

Boehmite and Vycor glass materials were used. Two pellets at each of three density levels of Boehmite, and two presumably identical Vycor pellets were studied. The Boehmite powder (see next section for properties) was compressed in a stainless steel ring to form pellets 12.7 mm. in thickness and 25.4 mm. in diameter. The ring and pellet as a unit were then installed in a stainless steel chamber (details in 8a, Figure 1) with O rings to obtain a tight seal. This arrangement was tested at pressures up to 15 atm.

The Vycor cylinders, 6.35 mm. in diameter, were cut to lengths of 14.4 mm. from number 7930 rod. Prior to installation the pellets were heated at 450°C. for 2 hr. to remove water. Then they were inserted in slightly undersize tygon tubing. The chamber (8b) was leak proof to 3-atm. pressure.

The nitrogen (99.99% purity) was used directly from the cylinder. The electrolytic hydrogen (99.7% purity) was passed through a Deoxo unit (3) and silica gel (4) to remove residual oxygen and water vapor.

Permeability

Prior to each permeability experiment, the pellet, in place in the apparatus, was degassed by flowing nitrogen through it for 12 hr. at 25°C. Total pressures were measured with gauges (6, 7) to 0.05 atm. For small pressure differences an oil manometer (5) was employed. The flow rate of nitrogen through the pellet was observed with soap-film meter (13), and the pressure on the downstream face (face 2) was adjusted by a valve in the exit line.

Diffusion and Flow

Without removing the pellet after permeability runs, nitrogen was supplied to face 1 of the chamber (high-pressure side) and hydrogen to side 2 for 2 hr. at 25°C. This period was sufficient to reach steady state for the diffusion and flow rates. With this arrangement there was flow and diffusion of nitrogen through the pellet from face 1 to face 2 and diffusion of hydrogen in the reverse direction.

The flow rates which ranged from 0.1 to 20 cc./sec. at 25°C., 1 atm. were measured in soap-film meters (13) and the gas composition was determined in thermal conductivity cell (12). The cell was immersed in a constant temperature bath of 25°C. and operated at a constant current of 160 mamp. Nitrogen was employed as the reference gas. From these results the flux of nitrogen and of hydrogen through the pellet was calculated for each set (P_1 and P_2) of pressures.

PROPERTIES OF BOEHMITE AND VYCOR

The equations for predicting the fluxes require void fractions and mean pore radii. Hence the physical measurements on the catalysts were directed towards this end.

Boehmite

The Boehmite powder was a spray-dried product.

After the diffusion measurements the pellets were broken into pieces. With these pieces, the volume and size distribution of the macro- and micropores were evaluated in a mercury porosimeter and sorptometer (continuous nitrogen adsorption). The porosimeter, with a maximum pressure of 5,000 lb./sq.in., was limited to pores of equivalent circular radii greater than 150 Å. Two samples of each pellet were analyzed in order to check the heterogeneity within a pellet and the porosimeter determination itself. Average deviations were about 10%.

Micropore properties are not sensitive to density changes so the sorptometer measurements were made for but one pellet at each density level. The sorptometer results scatter at high relative saturation pressures (p/p_o above 0.9, corresponding to equivalent radii greater than about 100 Å). This is probably due to saturation of the thermal conductivity cell with nitrogen. Hence the pore size distribution curves were drawn from the sorptometer data up to 100 Å and the region between 100 and 150 Å established by extrapolation of the porosimeter data. The sorptometer data in this region were higher than the extrapolated results, as noted by the dotted line in Figure 2 for pellet number 1-*a*. Since the volume of pores in this size interval is not large, the uncertainty in the curve between 100 and 150 Å is not significant. The relation between p/p_o and a for the nitrogen adsorption data is based upon the modified Kelvin equation as reported by Pierce (3).

The final pore size distribution curves obtained by differentiation of the cumulative pore volume curves for the various Boehmite pellets are shown in Figure 2. The pellet density, pore volume, surface area, and void fraction data could also be computed, and these are summarized in Table 1. The effect of increasing pellet density in reducing macropore volume, while micropore volume is rela-

TABLE 1. PROPERTIES OF BOEHMITE AND VYCOR

A. Boehmite powder*

S_g = 339 sq. m./g. Loss on heating = 24.9%
V_g = 0.80 cc./g. (Calcined at 1,100°F. for 1 hr.)

Particle size distribution:

Mesh no.	Size of opening, μ	% finer
100	149	87
270	74	48
325	44	35

B. Boehmite pellets†

Pellet no.	Pellet density, g./cc.	Mean pore radius $\bar{a}_a$, Å	Mean pore radius $\bar{a}_i$, Å	Pore volume, cc./g. V_{ga}	Pore volume, cc./g. V_{gi}	Pore volume, cc./g. V_g	Void fraction ϵ_a	Void fraction ϵ_i	Surface area S_g, sq. m./g.
1-*a*	0.658	5,400	27	0.759	0.40	1.16	0.499	0.263	300.
1-*b*	0.648	6,400	27	0.865	0.40	1.27	0.561	0.259	300.
2-*a*	0.942	1,400	25	0.404	0.38	0.784	0.382	0.358	307.
2-*b*	0.949	1,400	25	0.400	0.38	0.780	0.379	0.361	307.
3-*a*	1.215	660	24	0.172	0.37	0.542	0.209	0.450	310.
3-*b*	1.210	680	24	0.210	0.37	0.580	0.254	0.448	310.

C. Vycor**

Pellet density, g./cc.	Mean pore radius, Å	Pore volume, cc./g.	Porosity, ϵ_i	Surface area S_g, sq. m./g.
1.46	45	0.208	0.304	90

* Properties per gram of calcined powder.
† Properties per gram of degassed (25°C., with nitrogen flow for 12 hr.) pellet.
** Properties per gram of degassed (450°C., 2 hr.) pellet.

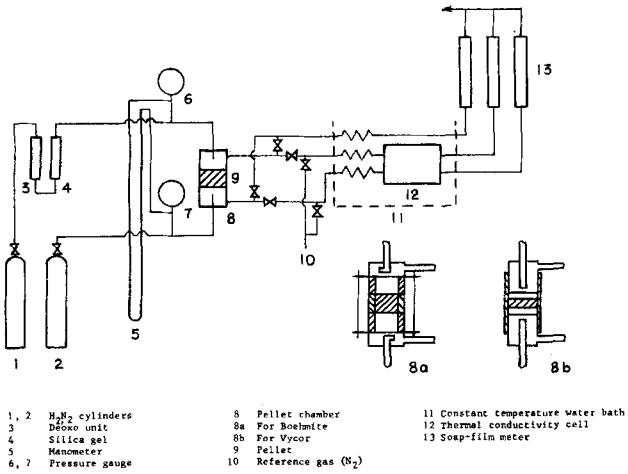

Fig. 1. Experimental apparatus.

tively unchanged, is clearly shown in Figure 2. These results suggest that little crushing of the powder particles occurred in the pelleting process. The assignment of pore volume to macro- or micropores was made by taking the boundary between the two kinds of pores at 100 Å. This radius corresponds approximately to the pores of minimum volume, as noted from Figure 2.

Mean pore radii for macro- and micropores are needed to evaluate diffusivities and Poiseuille flow terms in the equations presented later for predicting diffusion and flow rates. These were evaluated from the equations

$$\bar{a}_a = \frac{\int_{V_{g_i}}^{V_g} a_a dV_g}{V_g - V_{g_i}} \qquad (1)$$

$$\bar{a}_i = \frac{\int_{0}^{V_{g_i}} a_i dV_g}{V_{g_i}} \qquad (2)$$

The results are given in Table 1. Equations (1) and (2) represent correct averages for evaluating Knudsen diffusion. However, Poiseuille flow is proportional to a^2. However, as seen later, separate evaluation of $\bar{a}$ for each transport mechanism would introduce unjustified complexity into prediction methods.

The pellets prepared at the same density level were supposed to be identical. This was successful for pellets 2-*a* and 2-*b* but not for the others. The data for pellets 1-*a* and 1-*b* particularly show the sensitivity of ϵ_a and $\bar{a}_a$ to small differences in density. This sensitivity is an example of the difficulty in developing accurate methods of predicting flow and diffusion rates.

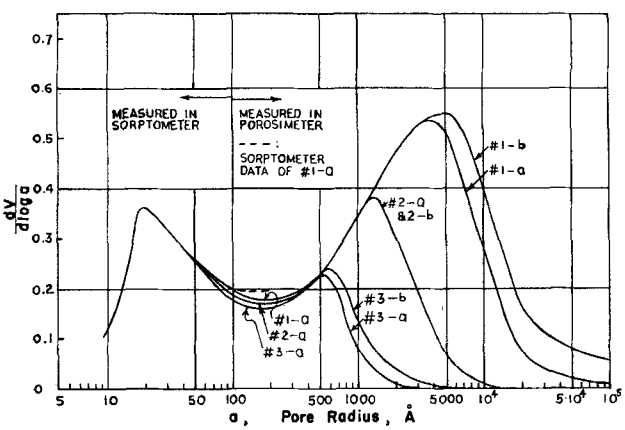

Fig. 2. Pore size distribution of Boehmite pellets.

Vycor

The properties of samples of Vycor from the same rod were available (2). These results, shown in Table 1, were used in the prediction methods considered later. No difficulty occurs in preparing two samples of Vycor of essentially identical properties.

RESULTS

Figures 3 to 8 and Table 2* illustrate the diffusion and flow rates for alumina pellets of each density level and for Vycor. The effect of the counter pressure gradient in suppressing the diffusion rate of hydrogen is clearly evident. This effect is greatest when the Poiseuille flow is large and when diffusion is in the bulk regime, as demonstrated by the data in Figure 3 for alumina pellet number 1. For this low density material the macropores are large enough ($\bar{a}_a$ = 5,400 Å from Table 1) that flow and diffusion are predominantly through these pores. Furthermore, the ratio of pore radius to mean free path is always greater than 5 so that diffusion occurs primarily by a bulk, rather than a Knudsen, mechanism. Figure 3 shows that the rate of diffusion of hydrogen decreases sharply (from the value at constant pressure) with increasing ΔP and approaches zero when the pressure drop across the pellet exceeds 2(0.2) or 0.4 atm.

In contrast, Vycor contains no macropores, and the mean pore radius (45 Å from Table 1) is so small that diffusion is almost entirely by collisions with the wall (Knudsen mechanism). Under these circumstances intermolecular collisions are unimportant, and the counter pressure gradient should have little effect on the diffusion of hydrogen. Figure 5 shows that this is exactly what happens: the diffusion rate at increasing ΔP values is not significantly changed from that at constant pressure.

Alumina pellets numbers 2 and 3 indicate the effect of decreasing macropore void fraction and mean radii. As the void fraction decreases, the fraction of the total dif-

* Tabular material has been deposited as document 8253 with the American Documentation Institute, Photoduplication Service, Library of Congress, Washington 25, D. C., and may be obtained for $1.25 for photoprints or $1.25 for 35-mm. microfilm.

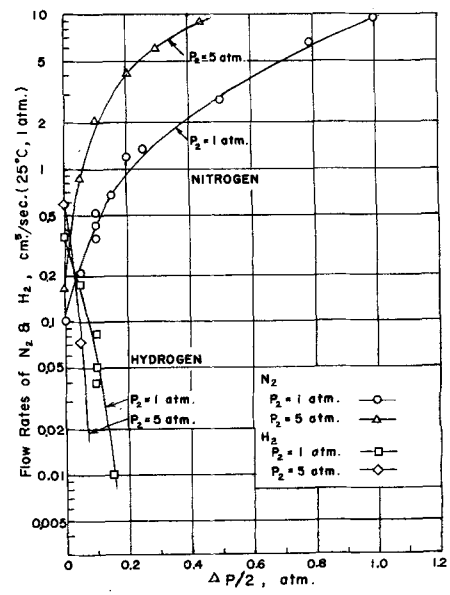

Fig. 3. Nitrogen and hydrogen flow rates, Boehmite pellet 1-a.

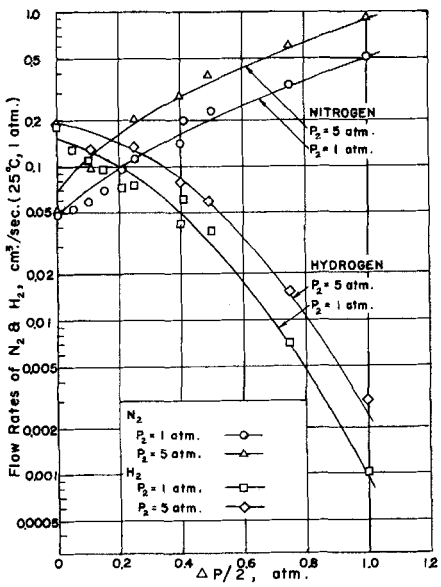

Fig. 4. Nitrogen and hydrogen flow rates, Boehmite pellet 2-a.

fusion rate through the micropores increases, and this must be of the Knudsen type because $\bar{a}_i = 24$ to 27 Å. Similarly, as $\bar{a}_a$ decreases, more of the transport in the macropores is by Knudsen diffusion. Both factors tend to reduce the effect of ΔP on N_{H_2} as shown by the data for these pellets in Figures 4 and 5.

The curves for nitrogen vary with ΔP in about the same way for all the catalysts. This is due to the fact that for Poiseuille flow, or bulk and Knudsen diffusion, the mass transfer rate is approximately proportional to ΔP. Thus whether the transport is primarily by Poiseuille flow, as in alumina pellet number 1 at high ΔP, or by Knudsen diffusion in Vycor, the same general effect of ΔP is observed.

Finally, it should be noted that the inverse molecular weight ratio is not a measure of N_{H_2}/N_{N_2} when there is a pressure gradient across the pellet. The data in Figures 3 to 5 show that N_{H_2}/N_{N_2} is about $(28/2)^{1/2} = 3.74$ at

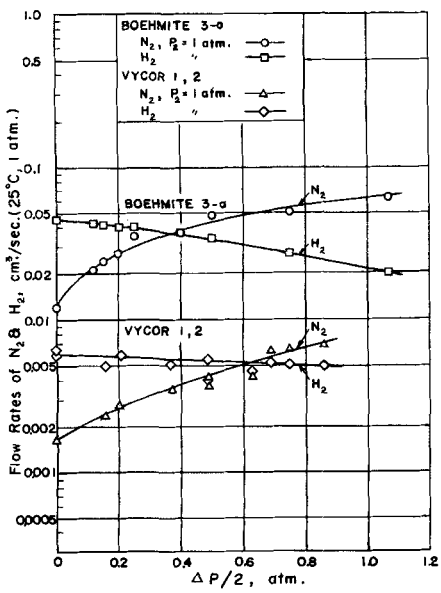

Fig. 5. Nitrogen and hydrogen flow rates for Boehmite 3-a and Vycor.

$\Delta P = 0$. However, as ΔP increases, this relationship does not apply.

PREDICTION METHODS

The pores of such materials as alumina and Vycor are infinitely complex, with varying and irregular shapes and sizes, partial and whole interconnections, some dead-end pores, and tortuous paths. An exact description appears impossible. Hence the development of an accurate method for predicting flow and diffusion rates is extremely difficult. One may adapt different approaches to the problem. One is to try and account for the complexities of the situation by using one kind of transport data to predict another. For example a prediction method for diffusion rates could be based upon experimental measurements of flow of a pure component with a pressure gradient. Another approach is to pose the objective of predicting both the diffusion and flow rates from only the easily measured physical properties of the porous material. The second method, while perhaps not giving as accurate results, has two distinct advantages: no arbitrary parameters, requiring transport data for their evaluation, are included, and the equations show more clearly the effects of the primary variables. This method is adopted here, treating the pure component and binary systems in sequence.

Permeability

For a pure component only the flow equations [Equations (19) and (20), Part I] are pertinent. These expressions for a single capillary can be integrated analytically across a capillary length L, taking the effect of pressure on D_{AA} into account. However, numerical calculations, even at the highest ΔP, show that a simpler integration, with average values of D_{AA} and P, gives results within 3% of those obtained from the rigorous solution. The simplified equations with the definition of the average quantities are

$$N_A = \frac{\bar{K}}{RT}\frac{\Delta P}{L} \tag{3}$$

$$\bar{K} = \frac{D_{KA}}{1 + D_{KA}/\bar{D}_{AA}} + \frac{1}{1 + \bar{D}_{AA}/D_{KA}}\left(\frac{\pi}{4}D_{KA} + \frac{a^2\bar{P}}{8\mu}\right) \tag{4}$$

$$\Delta P = P_1 - P_2 \tag{5}$$

$$\bar{P} = \frac{P_1 + P_2}{2} = P_2 + \frac{\Delta P}{2} \tag{6}$$

$$\bar{D}_{AA} = \frac{D_{AA_o}P_o}{\bar{P}} \tag{7}$$

For a bidisperse pore system the random pore model (4) supposes that the total flux is the sum of three contributions in parallel: through the macropores of effective area ϵ_a^2; through the micropores of area ϵ_i^2; and a macro-micro series mechanism of area $2\epsilon_a\epsilon_i^2/(1-\epsilon_a)$. Equation (4) can be applied to each contribution. The result analogous to the constant pressure diffusion case is

$$N_A = \left[\epsilon_a^2\bar{K}_a + \epsilon_i^2\bar{K}_i + \frac{4\epsilon_a\epsilon_i^3}{1-\epsilon_a}\bar{K}_i\right]\frac{\Delta P}{RTL} \tag{8}$$

The permeability for the macropores $\bar{K}_a$ is given by Equation (4) with $a = \bar{a}_a$ and with D_{KA} evaluated from the mean macropore radius $\bar{a}_a$; that is

$$\bar{D}_{KA_a} = \frac{2}{3}\bar{v}_A\bar{a}_a \tag{9}$$

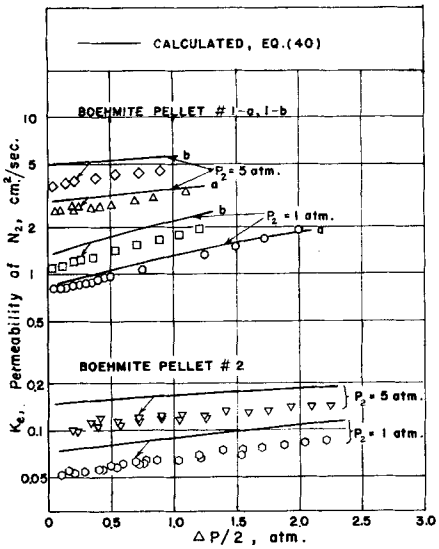

Fig. 6. Permeability results, Boehmite pellets numbers 1 and 2.

Similarly $\overline{K}_i$ is obtained from $\overline{D}_{KA_i}$, based upon $\overline{a}_i$.

Equation (8) provides a method for calculating the flow rate of a pure component from easily determined geometric properties (ϵ, $\overline{a}$) of the porous catalyst. Comparison of Equations (3) and (8) indicates that the transition from single capillary to porous media is simply made by replacing the capillary permeability $\overline{K}$ with an effective value

$$K_e = \epsilon_a^2 \overline{K}_a + \frac{\epsilon_i^2(1 + 3\epsilon_a)}{1 - \epsilon_a} \overline{K}_i \qquad (10)$$

The experimental permeability data are compared with the predictions from Equations (8) and (10) by plotting K_e vs. the pressure gradient across the pellet thickness. The experimental K_e values were obtained from observed data with Equation (3). Figures 6 and 7 show the results for the various solids. The observed K_e covers a range of 6,000-fold, from about 4 sq.cm./sec. for alumina pellet number 1-*b* at $P_2 = 5$ atm. down to 7×10^{-4} sq.cm./sec. for Vycor. Also the porous media vary from a low-density pellet, where the macropore contribution dominates the process, to Vycor in which there exists only micropores.

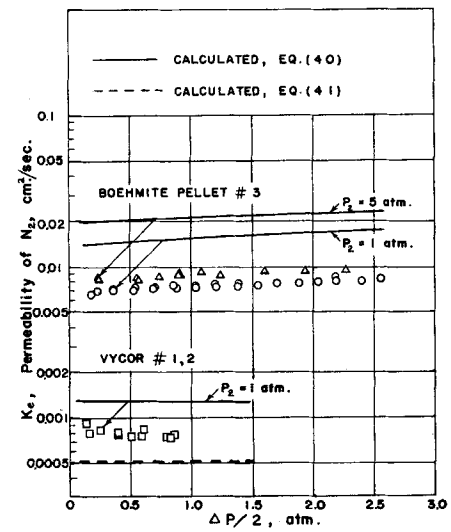

Fig. 7. Permeability results, Boehmite pellet number 3 and Vycor.

The predicted results follow closely the experimental data: they cover the same large range of values and show the same trend with ΔP. When one considers this and the fact that no arbitrary coefficients are involved in the prediction method, the agreement between observed and predicted permeabilities is considered excellent.

It may be noted that the increasing effect of ΔP on K_e in changing to materials with larger pores and larger void fractions is again due to the change from Knudsen transport in Vycor to Poiseuille flow and bulk diffusion in alumina pellet number 1.

In Figure 7 the dotted line shows the Vycor permeability predicted from Barrer's (*1*) flow data measured for a Vycor material with similar properties. The equation for K_e can be related to a tortuosity factor q

$$K_e = \frac{\epsilon_i}{q^2} \overline{K}_i \qquad (11)$$

with a parallel pore model. Barrer found $q = 2.56$ from flow measurements. The permeability $\overline{K}_i$ for the Vycor pores is obtained from Equation (4) with $\overline{a} = \overline{a}_i$. The dotted line does not represent a prediction method, since q was determined from experimental transport data. However, the data points and dotted line do measure the agreement between the flow data observed by Barrer and in this study. It is concluded, as is well known, that the permeability is a sensitive property of a porous material, and its accurate prediction is inherently difficult.

Diffusion and Flow

For a binary system the starting point is again the expressions for a single capillary. However, for this case both the equations for the net flux of A [Equations (8) and (14), Part I] and for the combined transport [Equations (15) and (16), Part I] are necessary in order to calculate N_A and N_B.

First the capillary equations are integrated over a length L. Then these results are adapted to a porous solid by introducing an effective flow parameter C_e and Knudsen diffusivities for the average macro- and micropore radii. The procedure is the same in principle as was used to adapt the permeability equations to a porous catalyst. In practice an analytical solution is not possible for a binary system, and also simple average values of y_A and P cannot be used. If flow rates are to be evaluated, a simultaneous, step-by-step numerical method is required for solution of the diffusion and combined transport equations. These differential equations for N_A and $mN_A + N_B$ are given in row 1, columns 3 and 4, of Table 3 for a single capillary, and in row 3 for a porous catalyst. A trial-and-error procedure is necessary when one assumes numbers for N_A and N_B and then evaluates the double assumption by comparing calculated and experimental values of y_A and P at the end of the pellet (at $x = L$).

This laborious procedure can be avoided by working with C_e because it is rather insensitive to variations in y_A and P. Arithmetic average values can be used with little error in integrating the single capillary equations in terms of an average $C = \overline{C}$. The appropriate expressions are given in row 2, column 4, of Table 3. The C_e for the catalyst pellet is related to $\overline{C}_a$ and $\overline{C}_i$ as shown in row 3, column 4. Thus C_e can be predicted from the pore geometry, just as K_e was calculated previously. The computed values then can be compared with an experimental C_e, obtained directly from the data using the equation in row 4, column 4.

The results are shown in Figures 8 and 9 plotted on coordinates similar to those in Figures 6 and 7 for permeability. In fact C_e may be regarded as the permeability

TABLE 3. EQUATIONS FOR DIFFUSION AND FLOW

Column no. →	2. Single component	3. Diffusion of A	4. Combined transport (flow equation)
Row 1 Differential equation for single capillary	$N_A = -\frac{K}{RT}\frac{dP}{dx}$, [Equation (19), Part I] $K = \frac{D_{KA}}{1+\frac{D_{KA}}{D_{AA}}} + \frac{1}{1+\frac{D_{AA}}{D_{KA}}}\left(\frac{\pi}{4}D_{KA} + \frac{a^2P}{8\mu}\right)$, [Equation (20), Part I]	$N_A = -\frac{1}{RT}\left[U\frac{d(Py_A)}{dx} + V\frac{dP}{dx}\right]$, [Equations (8) and (14), Part I] $U = \frac{D_{KA}}{1+[1+(m-1)y_A]\frac{D_{KA}}{D_{AB}}}$ $V = \frac{y_A}{\left(1+\frac{D_{AB}}{D_{KA}}\right)}\left\{\frac{a^2P}{8\mu} + \frac{\pi D_{KA}}{4[y_A+(1-y_A)/m]}\right\}$	$mN_A + N_B = -\frac{C}{RT}\frac{dP}{dx}$, [(Equation 15), Part I] $C = \frac{mD_{KA}}{1+[1+(m-1)y_A]\frac{D_{KA}}{D_{AB}}} + \left[\frac{my_A}{1+\frac{D_{AB}}{D_{KA}}} + \frac{1-y_A}{1+\frac{D_{AB}}{mD_{KA}}}\right]\times$ $\left\{\frac{\pi D_{KA}}{4[y_A+(1-y_A)/m]} + \frac{a^2P}{8\mu}\right\}$, [Equation (16) Part I]
2 Across capillary of length L	$N_A = \frac{\overline{K}}{RT}\frac{\Delta P}{L}$, [Equation (3)] $\overline{K} = \frac{D_{KA}}{1+\frac{D_{KA}}{\overline{D}_{AA}}} + \frac{1}{1+\frac{\overline{D}_{AA}}{D_{KA}}}\left(\frac{\pi}{4}D_{KA} + \frac{a^2\overline{P}}{8\mu}\right)$, [Equation (4)] $\overline{P} = \frac{1}{2}(P_1 + P_2)$ $\Delta P = P_1 - P_2$		$mN_A + N_B = \frac{\overline{C}}{RT}\frac{\Delta P}{L}$; $\overline{D}_{AB} = \frac{D_{AB_o}P_o}{\overline{P}}$ $\overline{C} = \frac{mD_{KA}}{1+[1+(m-1)\overline{y}_A]\frac{D_{KA}}{\overline{D}_{AB}}} + \left[\frac{m\overline{y}_A}{1+\frac{\overline{D}_{AB}}{D_{KA}}} + \frac{1-\overline{y}_A}{1+\frac{\overline{D}_{AB}}{mD_{KA}}}\right]\times$ $\left[\frac{\pi D_{KA}}{4[\overline{y}_A+(1-\overline{y}_A)/m]} + \frac{a^2\overline{P}}{8\overline{\mu}}\right]$ $\overline{y}_A = \frac{1}{2}(y_{A_1} + y_{A_2})$
3 Across bidisperse pellet (of length L)	$K_e = \epsilon_a^2\overline{K}_a + \frac{\epsilon_i^2(1+3\epsilon_a)}{1-\epsilon_a}\overline{K}_v$, × [Equation (10)]	$N_A = \frac{-1}{RT}\left[U_e\frac{d(Py_A)}{dx} + V_e\frac{dp}{dx}\right]$ $U_e = \epsilon_a^2\overline{U}_a + \frac{\epsilon_i^2(1+3\epsilon_a)}{1-\epsilon_a}\overline{U}_i$ $V_e = \epsilon_a^2\overline{V}_a + \frac{\epsilon_i^2(1+3\epsilon_a)}{1-\epsilon_a}\overline{V}_i$	$mN_A + N_B = \frac{C_e}{RT}\frac{\Delta P}{L}$ $C_e = \epsilon_a^2\overline{C}_a + \frac{\epsilon_i^2(1+3\epsilon_a)}{1-\epsilon_a}C_i$
4 Equations for experimental K_e and C_e	$(K_e)_{exp} = \frac{RTL}{\Delta P}N_A$		$(C_e)_{exp} = \frac{RTL}{\Delta P}(mN_A + N_B)$

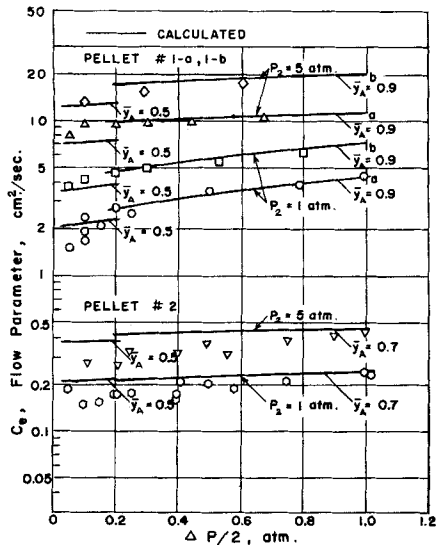

Fig. 8. Flow parameter for Boehmite pellets numbers 1 and 2.

of a binary system since it is a measure of the net transport of A and B. The range in C_e from Vycor to Boehmite pellet number 1 is several thousandfold, the same as observed for K_e, but the flow parameter is somewhat larger for the same conditions. The agreement between predicted and experimental results is better than for the pure component case and appears to be equally good for the entire range of pellets.

In the Knudsen regime, for example for Vycor and Boehmite pellet number 3, there is practically no effect of pressure on C_e, in agreement with the permeability results given in Figure 7. The influence of $\overline{y_A}$ is shown on the curves in Figure 8. For these two pellets the average composition deviated enough from 0.5 to indicate a significant effect. Predicted lines for the two extreme values of y_A are shown in the figure. The experimental points at the lowest ΔP correspond to $\overline{y_A} = 0.5$ and at $\Delta P/2$ above about 0.2, $\overline{y_A}$ approached the upper limit, 0.7 or 0.9. The predictions appear to represent correctly the effect of composition on the flow parameter.

For concise reference there is included also in Table 3, in the second column, the pure-component equations for a single capillary and porous pellet.

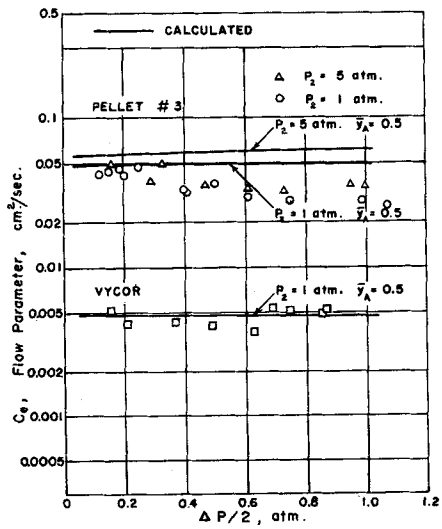

Fig. 9. Flow parameter for Boehmite pellets number 3 and Vycor.

SUMMARY

Diffusion rates through a porous catalyst, and counter to a pressure gradient, are severely suppressed with increasing gradient when the pores are large. For small pores, where the mass transport is by Knudsen flow, the pressure gradient does not affect the transport rate.

The random pore model, originally developed for constant pressure diffusion, provides a useful means for predicting the flow and diffusion characteristics of the catalysts studied. Results for binary systems can be interpreted in terms of a flow parameter which is analogous to the permeability for a pure component. This parameter, like the permeability, is very sensitive to pore size and void fraction but insensitive to the pressure gradient across the pellet.

ACKNOWLEDGMENT

The work was supported by a grant from the National Science Foundation.

NOTATION

A, B = gases A and B; nitrogen and hydrogen, respectively, in experimental work

$\overline{C}$ = average flow parameter over the length of a single capillary (see equation in column 4 of Table 3), sq.cm./sec.

D_{AB_o} = bulk diffusivity of A-B at reference pressure P_o, sq.cm./sec.

$\overline{D}_{KA}$ = Knudsen diffusivity of A evaluated for pore radius $\overline{a}$, sq.cm./sec.

C_e = average flow parameter for porous catalyst (see equation in Table 3, column 4), sq.cm./sec.

K = permeability; $\overline{K}$ = average value over the length of a single capillary, defined by Equation (4), sq.cm./sec.

K_e = average permeability for porous catalyst, defined by Equation (10), sq.cm./sec.

L = length of capillary or thickness of catalyst pellet, cm.

m = $(M_A/M_B)^{1/2}$

p/p_o = relative saturation pressure of nitrogen in helium-nitrogen stream to sorptometer

P_o = reference pressure at which D_{AB_o} is evaluated, atm.

q = tortuosity factor for porous catalyst, see Equation (11)

S_g = surface area of catalyst, sq.m./g.

V_g = pore volume of catalyst, cc./g.

$\overline{v}$ = mean molecular velocity, cm./sec.

y = mole fraction

ϵ = void fraction

Subscripts

a, i = macro- and micropores, respectively

1, 2 = high and low pressure ends of capillary (or faces of catalyst pellet), respectively; also nitrogen and hydrogen sides of pellet, respectively

LITERATURE CITED

1. Barrer, R. M., and J. A. Barrie, *Proc. Roy. Soc. (London)*, A213, 250 (1952).
2. Rao, M. R., and J. M. Smith, *A.I.Ch.E. Journal*, **10**, 293 (1964).
3. Pierce, C., *J. Phys. Chem.*, **57**, 149 (1953).
4. Wakao, N., and J. M. Smith, *Chem. Eng. Sci.*, **17**, 825 (1962).